ARKIV FÖR FYSIK Band 14 nr 20

Communicated 10 September 1958 by IVAR WALLER and KAI SIEGBAHN

Emission of charged $\Sigma+\pi$ from K^--proton capture in nuclear emulsions

By S. NILSSON and Å. FRISK

With 10 figures in the text

ABSTRACT

A 100 two-prong stars with charged baryon and π-meson only from K^- capture in nuclear emulsions have been analysed. 23 $\Sigma^+ + \pi^-$, 30 $\Sigma^- + \pi^+$ and 9 $\Sigma^\mp + \pi^\pm$ events were compatible with captures on bound and free protons. A comparison between the experimental and expected hyperon energy distribution, using a degenerate Fermi gas model of the nucleus, gives a best fit for an attractive real Σ-nuclear potential of 25 MeV. An average Coulomb potential of the capturing nucleus of 8 ± 2 MeV is deduced. The fraction of zero prong Σ^--stars is 0.66 ± 0.10. The Σ^--mass is found to be $m_{\Sigma^-} = 1196.7 \pm 0.6$ MeV from three K^- captures on free protons.

1. Introduction

The Σ-hyperon interaction with nuclei can be studied in two ways. The first method is to investigate the behaviour of the hyperon in a material for instance liquid hydrogen or emulsion. This method is at present restricted by the limited path length available. Another approach is to have a source of Σ-hyperons inside nuclear matter and to study how the Σ-nuclear interaction influences the observed quantities. In this case the creation process must be known as well as the properties of the nucleus.

The capture of negative K-mesons on complex nuclei in emulsion provides such a source. One type of event arising from K^- capture on bound protons permits a fairly clear interpretation. These are the stars with charged hyperon and π-meson only. Analysis of this type of event has been suggested by Gilbert, Violet and White [1] (hereafter referred to as GVW).

The following strong one-nucleon reactions conserving the baryon number, charge and strangeness are studied

$$K^- + p \rightarrow \Sigma^+ + \pi^- \quad \text{(A)}$$

$$\rightarrow \Sigma^- + \pi^+ . \quad \text{(B)}$$

In the present work 100 two-prong stars with charged baryon and pion only have been analysed. Parts 2 and 3 give the experimental details of the events with identified hyperon and pion. The events in which a baryon ends without producing secondary effects are treated in Parts 4 and 5. The hyperon and pion energy distributions are interpreted, using a degenerate Fermi gas model of the nucleus, in Part 6.

2. Details of the events with charged $\Sigma + \pi$

106 stars of a total of 818 K^- stars at rest in G5 emulsion had one prong $\geqslant 5\ \mu$m (due to a baryon), a π-meson track and no other prong $\geqslant 5\ \mu$m. "Along-the-track" scanning was used for finding the K^--stars. Details about the stacks and the acceptance criteria will be published in a paper on K^- interactions in flight [2].

Six of the 106 two-prong stars could not be completely analysed. The baryon from the remaining 100 events was identified as a Σ-hyperon in 52 cases. 10 Σ_ϱ^- were inferred from the analysis to be described later.

Details of the events with hyperon are given in Table 1. Three cases of B_ϱ + identified π^+ are also included. B_ϱ denotes a baryon prong ending without any secondary prongs or blobs.

The π-meson energies were determined by grain-counting. The procedure is described in a paper on K^- decay modes [3].

One of the main experimental problems encountered in the present investigation was to find a rapid and reliable way to estimate the ionisation of the baryon track. This had to be done in the cases, where a Σ decayed to a π-meson in order to identify the decays in flight.

The ionisation measurements were done by counting gaps. This is a rapid method, but it is subject to large subjective errors, if suitable precautions are not taken. To this end the following standard procedure was adopted. Before a series of measurements started a reference track was counted. Each track was counted by two observers and the mean, G, used as an estimate of the ionisation. The G-residual range relation was calibrated on stopping $\Sigma^+ \to p$ of different dip angles in the stacks. The effect of variations from glass to surface was eliminated by counting in the middle of the plates.

3. Free proton absorptions

The events 1974, 1269, 1771, 1113, 1899 and 1180 seem to form a well defined group. They are all colinear to within $\pm 1°$, with low residual momentum and with Σ and π energies in the region expected for K^- + free proton absorptions.

The Σ^- in 1113, 1899 and 1180 had a range of 690 ± 16, 691 ± 11 and $689 \pm 17\ \mu$m respectively. The characteristics of the endings were: 1 prong star, blob 2.2 μm and B_ϱ respectively. Using the known batch density and assuming the nominal emulsion thickness to be 600 μm the Σ^--mass is found to be $m_{\Sigma^-} = 1196.7 \pm \pm 0.6$ MeV. Range straggling and uncertainties in emulsion density and shrinkage factor are included in the error. The Σ^--tracks were flat and the uncertainty in the shrinkage factor can only introduce a negligible systematic error. Thus the events can safely be interpreted as free proton absorptions.

The situation is less clear with regard to the other three events. The Σ-hyperon in event 1771 very probably decayed in flight. The measured T_Σ was 13 ± 2 MeV

Table 1. Characteristics of the events with identified hyperon.

Event no.	Identification	Σ decay or capture[a]	Partner to hyperon	T_Σ, MeV[b]	T_π, MeV[b]	Angle between the Σ and π	Residual momentum MeV/c
1932	Σ^+	$p\,(r)$	π^-	15.5	35±1	151	114
1916	Σ^+	$p\,(r)$	π	13.5	59±1	141	115
1608	Σ^+	$p\,(r)$	π	19.0	73±3	134	156
1853	Σ^+	$p\,(r)$	π	14.5	61±6	122	165
2028	Σ^+	$p\,(r)$	π	8.2	80±7	118	163
1524	Σ^+	$p\,(f)$	π^-	29.5	50±1	128	213
1641	Σ^+	$p\,(f)$	π	33.0	57±3	79	337
1109	Σ^+	$p\,(f)$	π	28.5	55±4	135	192
1707	Σ^+	$\pi\,(r)$	π	32.5	32±2	35	366
1213	Σ^+	$\pi\,(r)$	π	27.0	69±6	134	185
1719	Σ^+	$\pi\,(r)$	π	12.3	72±5	120	167
1767	Σ^+	$\pi\,(r)$	π	27.6	55±3	141	177
233	Σ^+	$\pi\,(r)$	π	9.4	73±8	153	73
1807	Σ^+	$\pi\,(r)$	π	8.0	84±3	148	94
1971	Σ^+	$\pi\,(r)$	π	19.5	67±2	160	91
1994	Σ^+	$\pi\,(r)$	π	19.2	73±5	161	83
1370	Σ^+	$\pi\,(r)$	π	5.6	75±8	178	48
2192	Σ^+	$\pi\,(r)$	π	14.5	77±6	174	28
1577	Σ^+	$\pi\,(r)$	π	12.8	70±5	180	19
1974	Σ^+	$\pi\,(r)$	π	13.5	90±7	180	2
1269	Σ^+	$\pi\,(r)$	π	13.4	78±7	180	12
1037	Σ^+	$\pi\,(f)$	π^-	23±4	55±1	146	140
1942	Σ^+	$\pi\,(f)$	π^-	47±7	29±1	163	246
2083	$\Sigma^\pm$	$\pi\,(f)$	π	29±4	51±6	138	190
1045	$\Sigma^\pm$	$\pi\,(f)$	π	28±3	45±4	125	215
2111	$\Sigma^\pm$	$\pi\,(f)$	π	29±3	49±5	146	173
212	$\Sigma^\pm$	$\pi\,(f)$	π	35±5	52±4	165	167
1134	$\Sigma^\pm$	$\pi\,(f)$	π	25±3	51±3	140	168
1579	$\Sigma^\pm$	$\pi\,(f)$	π	5±2	75±6	180	57
1786	$\Sigma^\pm$	$\pi\,(f)$	π	41±6	36±2	103	305
1771	$\Sigma^\pm$	$\pi\,(f)$	π	13±2	94±7	180	10
130	$\Sigma^\pm$	i.i.f.	π	33±3	37±2	153	190
524	Σ^-	1.7, 1.3[c]	π	3.3	71±6	162	82
1187	Σ^-	5.6, 3.2	π i.f.	13.5	57±3	116	173
1813	Σ^-	6.0	π	6.3	82±5	157	84
1861	Σ^-	2.0	π	31.5	49±1	161	160
1977	Σ^-	1.6	π	2.7	80±3	118	151
1976	Σ^-	2.6	π	14.7	55±5	141	119
1168	Σ^-	170	π	18.1	55±2	123	177
1838	Σ^-	blob + electron	π	16.5	71±6	126	168
1862	Σ^-	2.1	π	3.5	73±5	116	145
2020	Σ^-	6145, 610, 226	π	21.4	57±3	128	178
1714	Σ^-	71.5	π	8.8	62±5	135	115
1345	Σ^-	63, 134, 1094	π	1.5	38±3	55	149

Table 1 (*continued*).

Event no.	Identification	Σ decay or capture[a]	Partner to hyperon	T_Σ, MeV[b]	T_π, MeV[b]	Angle between the Σ and π	Residual momentum MeV/c
1929	Σ^-	3.2, 1.6	π	5.8	52±2	89	177
1934	Σ^-	2220, 1.2	π	25.0	57±4	145	155
2150	Σ^-	7.3, 9.8	π	13.4	63±4	147	98
1159	Σ^-	1.3, 1.3	π	1.5	91±7	71	208
2188	Σ^-	3820, 631, 208, 1.6, 119, 1.6	π^+	20.4	55±1	159	107
1113	Σ^-	2.2	π	12.6	80±8	180	5
1899	Σ^-	5.0	π	12.6	84±4	180	0
1180	B_ϱ		π	12.6	88±8	180	5
834	B_ϱ		π^+	19.5	37±1	133	164
2123	B_ϱ		π^+	12.1	50±1	136	120
1940	B_ϱ		π^+	5.7	28±1	122	104

[a] $p\,(r)$: $\Sigma \rightarrow p$ at rest $\pi\,(r)$: $\Sigma \rightarrow \pi$ at rest
$p\,(f)$: $\Sigma \rightarrow p$ in flight $\pi\,(f)$: $\Sigma \rightarrow \pi$ in flight.
[b] Kinetic energy at the K^- capture point.
[c] Ranges of secondary prongs or blobs in μm.

whereas from range $T_\Sigma = 10.5$ MeV. In event 1974 and 1269 the Σ-hyperon was at rest within the limits of the measurements. The ranges were 781±20 and 780±22 μm respectively. This is two standard deviations away from the expected range of about 820 μm. Both tracks were steep, 39° and 46° respectively, in unprocessed emulsion. The explanations may be (i) the events are not K^- + free p absorptions, (ii) the small ranges are due to range straggling fluctuations, (iii) the measured ranges contain a systematic error, if the nominal thickness is not 600 μm at the point in question, (iv) the hyperon decays in flight near the end of its range. All explanations are possible and no decision can be made. They are not included in the following analysis due to their special characteristics. This omission has no influence on the results.

4. Energy balance considerations

Energy conservation between the initial and final state in the capture processes A and B implies [1] that

$$m_{K^-} + {}^{A}_{Z}X \rightarrow {}^{A-1}_{Z-1}X^* + m_\Sigma + m_\pi + T_\Sigma + T_\pi \tag{1}$$

if the K^- is captured at rest.

${}^{A}_{Z}X$ = the total energy of the initial nucleus in its ground state
${}^{A-1}_{Z-1}X^*$ = the total energy of the excited residual nucleus
T = the kinetic energies in the lab. system.

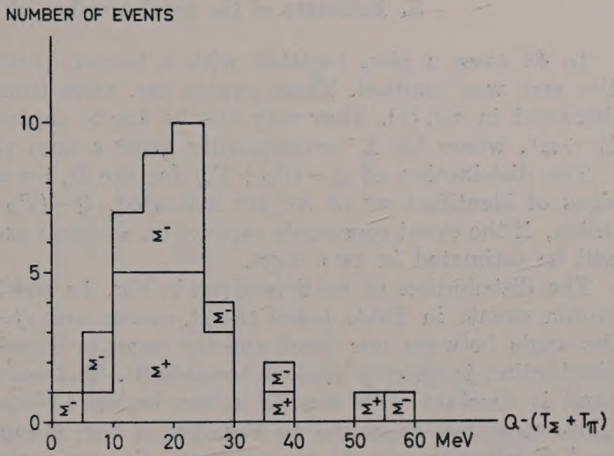

Fig. 1. The distribution of $E_{\text{ex}}+$ $+E_B=Q-(T_\Sigma+T_\pi)$ for the events with identified hyperon.

Further the excitation energy is

$$E_{\text{ex}}={}^{A-1}_{Z-1}X^*-{}^{A-1}_{Z-1}X,$$

the separation or binding energy of the last proton

$$E_B={}^{A-1}_{Z-1}X-{}^{A}_{Z}X+m_p$$

and the Q-value for the reactions (A) and (B)

$$Q=m_{K^-}+m_p-(m_\Sigma+m_\pi).$$

Equ. (1) may then be written

$$T_\Sigma+T_\pi=Q-(E_{\text{ex}}+E_B). \tag{2}$$

The Q-value is taken as 103 MeV for the reaction (A) and 96 MeV for the reaction (B) [4].

The quantity $Q-(T_\Sigma+T_\pi)$ is plotted in Fig. 1 for the events with identified Σ (Table 1), which are not reactions with free hydrogen. $Q-(T_\Sigma+T_\pi)$ is positive in all cases, which means that the events are consistent with the reactions (A) and (B) with respect to energy conservation. The mode value of $E_{\text{ex}}+E_B$ is

$$E_{\text{ex}}+E_B\sim 20 \text{ MeV}.$$

The spread in the $E_{\text{ex}}+E_B$ is to be expected from the statistical nature of the excitation process and the errors in determining T_Σ and T_π. The total charge of the $(\Sigma\pi)$-system was zero in all cases where both signs could be determined. Consequently all the events in Table 1 have been interpreted as arising from capture on bound or free protons. If the sign of the charge of one particle was determined, the sign of the charge of its partner was inferred from (A) or (B).

5. Estimate of the total number of Σ^--hyperons

In 48 cases a pion together with a baryon producing no secondary effects at the end was emitted. These events can arise from many possible reactions as discussed in ref. [1]. They may also be due to captures on bound protons yielding $\Sigma^- + \pi^+$, where the Σ^- subsequently gives a zero prong star.

The distribution of $Q - (T_B + T_\pi)$ for the $B_\varrho + \pi$ events is shown in Fig. 2. The signs of identified π^- or π^+ are indicated. $Q - (T_B + T_\pi) > 0$ is a necessary condition, if the event represents capture on a bound proton. The fraction of $\Sigma^- + \pi^+$ will be estimated in two ways.

The distribution of $\cos\theta$ is given in Fig. 3 *a* and 3 *b* respectively for the bound proton events in Table 1 and the B_ϱ events with $Q - (T_B + T) > 0$. θ is defined as the angle between one track and the negative direction of the other. The $\cos\theta_{\Sigma\pi}$ distribution is sharply peaked towards 0°. The $\cos\theta_{B\pi}$ distribution on the other hand is constant with a peak in the region $1 > \cos\theta_{B\pi} \geqslant 0.4$, where most of the ($\Sigma\pi$)-events fall according to Fig. 3 *a*. If the B and π prongs are unrelated their $\cos\theta$ distribution should be constant. One may therefore, as suggested by the Göttingen group [5], interpret the $\cos\theta_{B\pi}$ distribution as consisting of a $\cos\theta_{\Sigma\pi}$ distribution superimposed on a constant distribution arising from unrelated $B + \pi$ prongs.

Subtracting the uniform background we are left with 10 $\Sigma^- + \pi^+$.

This number can be estimated in another way. Assuming all B_ϱ + identified π^+ with $Q - (T_B + T_\pi) > 0$ to be $\Sigma^- + \pi^+$ and the same proportion of the $\pi^\pm$ to be π^+ as for the events with stopped π, there are $3 + \frac{3}{8} \times 19 \approx 10$ $\Sigma^- + \pi^+$ events.

The two independent estimates give the same result and 10 Σ_ϱ^- is taken as a reasonable figure. The three events with B_ϱ + identified π^+ are included in Table 1.

The ratio $\Sigma^- : \Sigma^+$ outside the nucleus can now be estimated. The decays $\Sigma^\pm$ in flight have about equal probability of being a Σ^- or a Σ^+. The hyperon interacting in flight is also divided into half a Σ^+ and half a Σ^-.

The result is

$$r = \frac{N(\Sigma^-)}{N(\Sigma^+)} = \frac{31}{25} = 1.24 \pm 0.34.$$

The prong distribution of the Σ^- endings can also be obtained. It is shown in Fig. 4. The fraction of Σ_ϱ^- is 0.66 ± 0.10.

6. The hyperon and pion energy distributions

The kinetic energies of the particles inside and outside the nucleus are related by

$$T_\alpha^{\text{in}} = T_\alpha - V_{N\alpha} - V_c. \tag{3}$$

α stands for Σ^+, Σ^-, π^+ or π^-. $V_{N\alpha}$ = the real nuclear potential felt by the particle. $V_{N\alpha}$ is positive for a repulsive and negative for an attractive potential. V_c = the Coulomb potential at the nuclear surface.

The total energy available for the ($\Sigma\pi$)-system inside the nucleus is

$$U^{\text{in}} = m_\Sigma + m_\pi + T_\Sigma^{\text{in}} + T_\pi^{\text{in}}$$

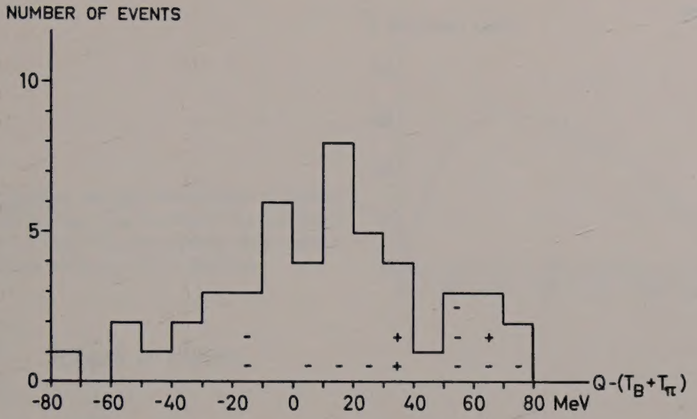

Fig. 2. The distribution of $E_{\text{ex}} + E_B = Q - (T_B + T_\pi)$ for the events with zero prong baryon ending.

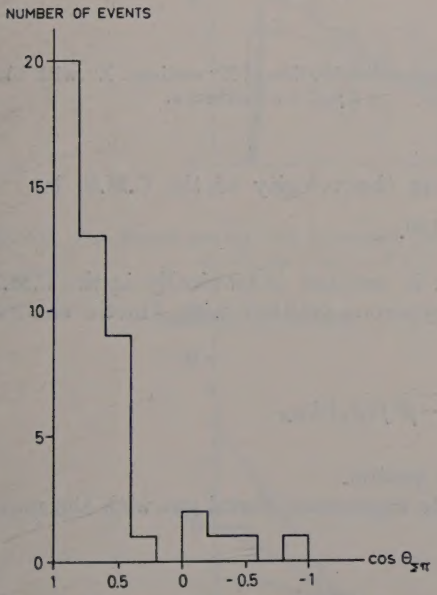

Fig. 3 *a*. The distribution of $\cos\theta_{\Sigma\pi}$ for all events with identified hyperon. $\theta_{\Sigma\pi}$ = the space angle between one track and the negative direction of the other.

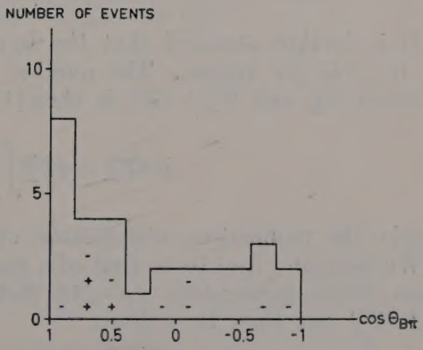

Fig. 3 *b*. The distribution of $\cos\theta_{B\pi}$ for the events with zero prong baryon ending and $Q - (T_B + T_\pi) > 0$. Events with associated positive π-meson are marked +, with negative −.

which can be written by means of equ. (2) and (3)

$$U^{\text{in}} = m_\Sigma + m_\pi + Q - (V_{N\Sigma} + V_{N\pi}) - (E_{\text{ex}} + E_B). \tag{4}$$

The following interaction model will be chosen in order to obtain the expected energy distribution of the hyperon. The K^- is captured by a proton with the momentum p_N inside the nucleus. Assuming that the total momentum of the

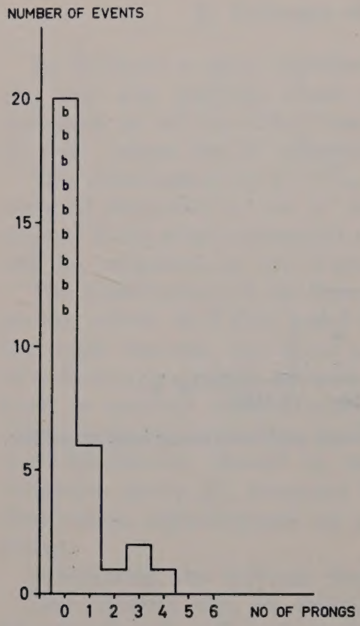

Fig. 4. The prong distribution of Σ^- endings. Σ^- with blob $< 5\ \mu$m are marked *b*.

$(K^- p)$ system equals the proton momentum the velocity of the C.M.S. is

$$\beta = p_N / U^{\text{in}}.$$

It is further assumed that the hyperon is emitted isotropically in the C.M.S. of the $(K^- p)$ system. The number of hyperons emitted with kinetic energies between T_Σ^{in} and $T_\Sigma^{\text{in}} + dT_\Sigma^{\text{in}}$ is then [1]

$$F\, dT_\Sigma^{\text{in}} \propto dT_\Sigma^{\text{in}} \int \frac{1}{\beta} \sqrt{1-\beta^2}\, f(p_N)\, d p_N$$

$f(p_N)$ = the momentum distribution of the proton.

We assume $f(p_N)$ to be that of a complete degenerate Fermi gas with the maximum Fermi momentum $p_F = 215$ MeV/c.

$F\, dT_\Sigma^{\text{in}}$ can then be written

$$F\, dT_\Sigma^{\text{in}} \propto \{(1-\beta_{\text{min}}^2)^{3/2} - (1-\beta_{\text{max}}^2)^{3/2}\}\, dT^{\text{in}}, \tag{5}$$

where β_{min} and β_{max} are obtained from

$$m_\Sigma + T_\Sigma^{\text{in}} = (E_\Sigma^* + p_\Sigma^* \beta_{\text{min}}) \frac{1}{\sqrt{1-\beta_{\text{min}}^2}}, \tag{6}$$

$$m_\Sigma + T_\Sigma^{\text{in}} = (E_\Sigma^* - p_\Sigma^* \beta_{\text{max}}) \frac{1}{\sqrt{1-\beta_{\text{max}}^2}}.$$

E_Σ^* and p_Σ^* are the total hyperon energy and momentum in the $(\Sigma\pi)$ C.M.S. β_{max} is subject to the restriction $\beta_{\text{max}} \leqslant p_F / U^{\text{in}}$.

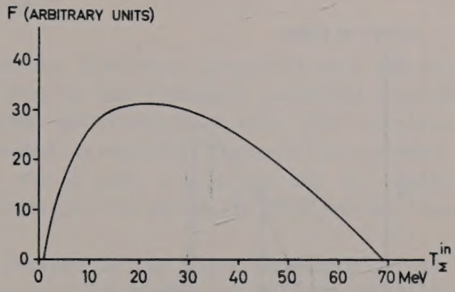

Fig. 5. The hyperon energy distribution inside the nucleus assuming the nucleon momentum distribution to be that of a complete degenerate Fermi gas with $p_F = 215$ MeV/c.

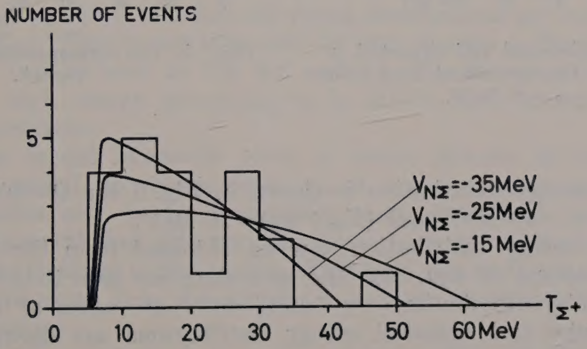

Fig. 6 *a*. The experimental and expected Σ^+ energy distribution. The theoretical curves are shown for $V_{N\Sigma^+} = V_{N\Sigma^-} = -15, -25$ and -35 MeV.

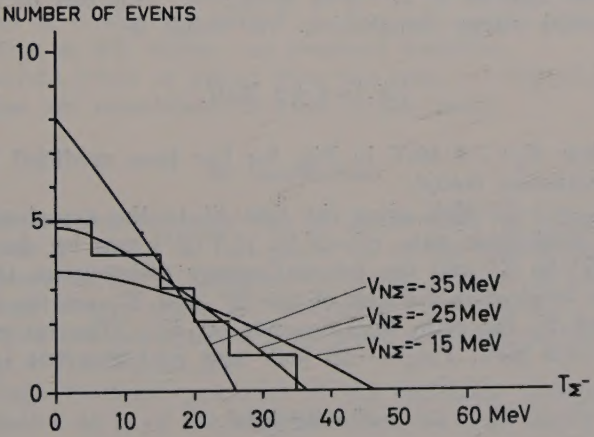

Fig. 6 *b*. The corresponding distributions for Σ^-.

The Σ^+ and Σ^- internal energy distributions will be the same provided $(E_{ex} + E_B)_+ = (E_{ex} + E_B)_-$ and $V_{N\Sigma^+} = V_{N\Sigma^-}$. This has been assumed and the small difference due to the difference in Q-value has been neglected.

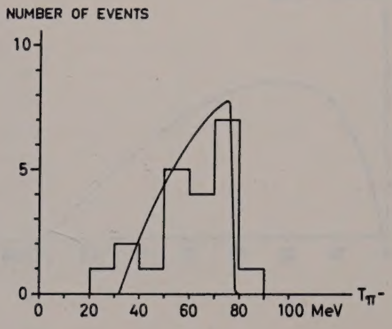

Fig. 7 *a*. The experimental and expected π^- energy distribution. The theoretical curve refers to $V_{N\Sigma} = -25$ MeV.

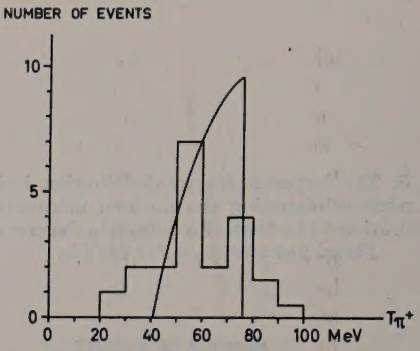

Fig. 7 *b*. The corresponding distributions for π^+.

The internal energy distribution is shown in Fig. 5 for $Q = 100$ MeV, $V_{N\Sigma} = -25$ MeV, $V_{N\pi} = -40$ MeV and $(E_{ex} + E_B) = 20$ MeV.

The external energy distribution can be obtained from the internal energy distribution by means of equ. (3). The procedure has been to obtain the best fit to the experimental distributions by taking different values of $V_{N\Sigma}$.

The experimental and expected energy distributions are shown in Fig. 6 *a* for Σ^+ and Fig. 6 *b* for Σ^-. The curves have in each case been normalized to the number of events in the histogram. The value $|V_c| = 8$ MeV has been used. It has been deduced from the fact that the number of Σ^+ with energy $> 2|V_c|$ is equal to half the number of Σ^- with energy > 0. This can be seen from equ. (3) and the internal energy distribution. The result is

$$|V_c| = 8 \pm 2 \text{ MeV}.$$

The part below $T_{\Sigma^+} = 8$ MeV in Fig. 6 *a* has been modified by taking into account the penetration factor.

The value $V_{N\Sigma} = -25$ MeV gives the best fit to the experimental data.

The internal production rate $r^{in} = N(\Sigma^-)/N(\Sigma^+)$ can be obtained from the external ratio Σ^- to Σ^+ and the internal energy distribution. One has also to assume that the total cross sections of the Σ^+ and Σ^- are the same in nuclear matter. For fixed V_c the ratio then depends on $V_{N\Sigma}$. The internal ratio corresponding to $|V_c| = 8$ MeV, $V_{N\Sigma} = -25$ MeV and $r = 1.24 \pm 0.34$ is

$$r^{in} = 2.3 \pm 0.6.$$

The expected π-meson distributions have been obtained from the corresponding Σ distributions by means of equ. (2) using $E_{ex} + E_B = 20$ MeV. The curves are given together with the experimental histograms in Fig. 7 *a* for π^- and 7 *b* for π^+. Only the curves for $V_{N\Sigma} = -25$ MeV are shown. The model reproduces the experimental data fairly well.

7. Discussion

The conclusions about the magnitude of the Σ-nuclear potential and the depletion of the number of emerging Σ^- due to the Coulomb potential depend to a large extent on the nucleon momentum distribution chosen. One common conclusion seems, however, to be well founded: a repulsive potential is excluded. A repulsive potential as low as $+10$ MeV would give a peak in the Σ^+ distribution around 20 MeV and extend the energies to about 65 MeV, which has no support in the experimental data.

A Gaussian momentum distribution as treated in the paper by Capps [6] permits no decision between for instance $V_{N\Sigma} = -15$ MeV and $V_{N\Sigma} = -25$ MeV. The fit between the expected and experimental distributions is improved by choosing the higher value, but the calculated distributions are very insensitive to the value of $V_{N\Sigma}$. This is not the case, if one chooses a Fermi gas model of the nucleus as can be seen in Fig. 6 *a* and 6 *b*. The Gaussian distribution also gives a tail of high energy extending up to 60–70 MeV, which has no experimental correspondence.

The Gaussian model generally gives a better picture of the reality than the Fermi gas model. In the present case it does not give any improvement. One of the reasons may be the assumption made in both the present treatment and the references [1] and [5], that the total momentum of the (K^-p)-system is equal to the momentum of the proton. This need not be true and if the nucleon and K^- momenta come into the picture in a more complicated way the distributions may change.

The ratio $\Sigma^- : \Sigma^+$ is about $2:1$ in K^- captures on free protons. The external ratio $r = 1.24 \pm 0.34$ is within the limits consistent with an internal production ratio $r^{\text{in}} = 2$. The ratio $r^{\text{in}} = 2$ would require $V_{N\Sigma} = -18$ MeV to give $r = 1.24$. With the present model the difference between $r^{\text{in}} = 2$ and r can be explained by the influence of Coulomb potential. A Gaussian model gives for $r^{\text{in}} = 2$ the ratio $r \sim 1.4$, which is still within one standard deviation.

The ratio $r = 1.24 \pm 0.34$ is higher than the ratio $r = 0.83 \pm 0.25$ obtained by GVW. The values are reconcilable in view of the errors.

8. Conclusions

The results of the present paper can be summarized as follows.

(i) The ratio of Σ^- to Σ^+ is 1.24 ± 0.34 for events with charged hyperon and π-meson only produced by K^- capture on bound protons in nuclear emulsions.

(ii) The fraction of zero prong Σ^- endings is 0.66 ± 0.10.

(iii) The mass of the Σ^- hyperon from three $K^- +$ free $p \rightarrow \Sigma^- + \pi^+$ events is found to be $m_{\Sigma^-} = 1196.7 \pm 0.6$ MeV.

(iv) The average Coulomb potential of the capturing nucleus is 8 ± 2 MeV. This indicates that $\sim 40\,\%$ of the captures occur on light nuclei and $\sim 60\,\%$ on heavy nuclei.

(v) The experimental hyperon energy distributions have been fitted by an interaction model assuming a Fermi momentum distribution of the bound proton. The theoretical distributions are quite sensitive to the assumed value of the Σ-nuclear potential. The best agreement is obtained for an attractive potential $V_{N\Sigma} = -25$ MeV.

(vi) On the basis of the above model the decrease of an assumed internal Σ^-/Σ^+ ratio of about 2 to the external ratio 1.24 can be explained by the inhibition of emerging Σ^- relative to the Σ^+ by the difference in Coulomb potential.

ACKNOWLEDGEMENTS

We want to thank Professor E. J. Lofgren for his kind cooperation and Dr. G. Ekspong and Professor G. Goldhaber for exposing and the Bristol and Berkeley groups for processing the stacks. Special thanks are due to Dr. G. Ekspong for his constant encouragement, illuminating discussions and invaluable advice. Professor K. Siegbahns support of this work is gratefully acknowledged.

We are indebted to the Air Research and Development Command through its European Office, which has partly sponsored this work. Thanks are due to the Swedish Atomic Energy Commission for financial support.

Institute of Physics, University of Uppsala, Uppsala, Sweden

REFERENCES

1. F. Gilbert, C. Violet, and S. White: Phys. Rev. *107*, 228 (1957).
2. S. Nilsson and Å. Frisk: Arkiv f. Fysik 14, 277 (1958).
3. S. Nilsson and Å. Frisk: Arkiv f. Fysik 14, 293 (1958).
4. W. H. Barkas and A. H. Rosenfeld: UCRL-8030 (1958).
5. Proc. of the VII Rochester Conf., VI-16 (1957).
6. R. H. Capps: Phys. Rev. *107*, 239 (1957).

Tryckt den 24 september 1958

Uppsala 1958. Almqvist & Wiksells Boktryckeri AB